Electronic Properties of Adsorption Nitrogen Monoxide on Inside and Outside of the Armchair Single Wall Carbon Nanotubes: A Density Functional Theory Calculations

A. Abbas Rafati,*,† S. Majid Hashemianzadeh,‡ and Z. Bolboli Nojini†

Faculty of Chemistry, Bu-Ali Sina University, Hamedan, Iran, and College of Chemistry, Iran University of Science and Technology, Tehran, Iran

Received: October 12, 2007; In Final Form: December 12, 2007

Density functional theory (DFT) was used to study the adsorption of nitrogen monoxide (NO) on the armchair (4, 4), (5, 5), (6, 6), and (7, 7) carbon nanotubes. The effect of molecular orientation on the adsorption process was also studied. Both the external (two modes, N-down and O-down; NO molecular axis perpendicular to the C atoms of the nanotubes) and internal (one mode, NO molecular axis perpendicular to the *z* axis of a nanotube) adsorption orientations were studied. The adsorption energies, equilibrium distances, highest-occupied molecular orbital−lowest-unoccupied molecular orbital energy gap, and partial charges of the C atoms were also found. The global indices were calculated using the Kopmann's theorem. Computational results show that NO molecules are physisorbed on both sites (external and internal) of the nanotubes; for the O-down mode, the NO molecules were strongly physisorbed. Stability of tube−molecule for the adsorption of NO molecules on the outer wall of a nanotube decreases as the tube diameter increases. In contrast, NO penetration into a nanotube increases as the tube diameter increases. The results show that NO molecules cannot be adsorbed on the inner walls of the nanotubes with diameters lower than 5.38 Å. Finally, physisorption of the NO molecules via the oxygen head (the O-down mode) was stronger than the other adsorption mode.

Introduction

In the recent years, carbon nanotubes have been intensively studied due to their importance as building blocks in nanotechnology.[1−3] They not only have outstanding mechanical and electronic characteristics but also hold considerable promise as molecular containers with applications such as hydrogen fuel cells,[4,5] nanoelectronic devices, chemical probes, and biosensors.[6−9] The key element that makes nanotubes so potentially useful as electrochemical storages is their structure.[10] Recent studies have shown that the physical properties of single-wall carbon nanotubes (SWNTs) could be modified by adsorption of foreign atoms or molecules.[11−13] Gas adsorption on carbon nanotubes is an important issue for both the fundamental research and technical applications of nanotubes. Selective reduction of nitrogen monoxide (NO) in oxidizing atmosphere has recently received much attention because it has a potential as a practical measure to remove NO_x emitted from diesel lean burn engines.[14] Some researchers have found that exposure to O_2, NO_2, or NH_3 dramatically influences the electrical resistance and thermoelectric power of semiconducting SWNTs.[11,12] Several experimental workers have shown that the electronic and transport properties of carbon nanotubes are extremely sensitive to oxygen exposure.[11,12,15] On the theoretical side, many calculations and analyses with different levels of sophistication have been reported.[16−24] Also, Kyotani and Tomita[25] have studied chemisorptions of NO and N_2O molecules on both the zigzag and armchair edges. Yates et al.[26] have also studied the adsorption and dimerization of NO molecules on the inside of the SWNTs by IR spectroscopy. Many studies have been carried out on various types of reductants for the selective catalytic reduction of NO.[27−30] Currently, there is no report on the adsorption of NO molecules on nanotubes. Therefore, to understand the effect of NO molecules on the electronic and transport properties of carbon nanotubes, we theoretically studied adsorption of NO molecules on the armchair SWNTs.

The DFT[31] has been successful in rationalizing popular concepts such as chemical reactivity and selectivity of molecules based on their global and local reactivity indices. The global index includes electronegativity[32,33] (χ) and hardness[32,34,35] (η), while the local index includes the Fukui function[36] ($f(r)$ and ($s(r)$). Pauling introduced the concept of electronegativity as the power of an atom in a molecule to attract electrons to itself.[37] The idea of hardness was given by Pearson in the context of hard−soft acid−base (HSAB)[38] principle, which states that "hard likes hard and soft likes soft". Another hardness-based principle is the maximum hardness principle (MHP), which states that[35,41] "there seems to be a rule in nature according to which molecules arrange themselves so as to be as hard as possible."[39,40] For an *N*-electron system with a total energy (E) and external potential $\upsilon(r)$, electronegativity[32] (χ) and hardness[35] (η) are defined as the following first-order[42] and second-order[43] derivatives, respectively

$$\chi = -\left(\frac{\partial E}{\partial N}\right)_{\upsilon(r),T} = -\mu \tag{1}$$

$$\eta = \frac{1}{2}\left(\frac{\partial^2 E}{\partial N^2}\right)_{\upsilon(r),T} = \frac{1}{2}\left(\frac{\partial \mu}{\partial N}\right)_{\upsilon(r),T} \tag{2}$$

where μ is the electronic chemical potential that is defined as the negative of the electronegativity. In addition the global softness, S, of the equilibrium state of an electronic system at temperature T is defined by[31]

* To whom correspondence should be addressed. Phone: ++98-811-828 2807. Fax: ++98-811-825 7407. E-mail: rafati_aa@yahoo.com.
† Bu-Ali Sina University.
‡ Iran University of Science and Technology.

10.1021/jp709955g CCC: $40.75
Published on Web 02/19/2008

$$S = \frac{1}{2\eta} = \left(\frac{\partial N}{\partial \mu}\right)_{v(r),T} \tag{3}$$

Parr and his co-workers[44] have recently introduced an electrophilicity index (w), as

$$w = \left(\frac{\mu^2}{2\eta}\right) \tag{4}$$

which was proposed as a measure of the electrophilic power of a molecule.

In this work, we used the DFT calculations to study the adsorption of NO on various adsorption sites of four armchair (4, 4), (5, 5), (6, 6), and (7, 7) carbon nanotubes such as the inside and outside of the nanotubes. Also two orientations of NO molecules on the outside of the tubes, N-down and O-down, modes were considered. For the N-down and O-down modes, the NO bond axis is perpendicular to the C atoms of the SWNTs. In the case of the inside of the SWNTs, the NO bond axis is perpendicular to the z axis of the tubes. Three ways of approaches (N-down, O-down, and inside of the tubes) were considered for the armchair (4, 4), (5, 5), (6, 6), and (7, 7) carbon nanotubes. The equilibrium geometry, adsorption energy, charge transfer, and electronic properties were calculated using the Gaussian 2003 package.[45]

Computational Method

We used the DFT to investigate the structural and electronic properties of the tube−molecule systems during the adsorption of NO molecule on SWNTs. Single-point (SP) calculations were carried out in all cases with the B3LYP/3-21G** level of theory. A carbon nanotube of achiral type (armchair) was studied in this work, considering an average diameter within 5−9 Å for the SWNTs. One-dimensional periodic boundary condition was applied along the tube axis. For all the tubes, we used one NO molecule per unit cell in the tube axis direction. In addition, for all the tubes, the number of cells was 10. In this case, the number of atoms per tube for the (4, 4), (5, 5), (6, 6), and (7, 7) nanotubes were 160, 200, 240, and 280, respectively. For SWNTs, calculations were carried out to obtain the adsorption energy curves (Figure 1) as well as the equilibrium tube−molecule distance for each system. We also examined the adsorption energy curves with the Lennard-Jones and Kihara potential equations (eqs 5 and 6) to obtain the parameters of these potentials (ϵ, σ, and δ)

$$u(r) = 4\epsilon\left[\left(\frac{\sigma}{r}\right)^{12} - \left(\frac{\sigma}{r}\right)^{6}\right] \tag{5}$$

$$u(r) = 4\epsilon\left[\left(\frac{\delta - d}{r - d}\right)^{12} - \left(\frac{\delta - d}{r - d}\right)^{6}\right] \quad r > d \tag{6}$$

where ϵ is an attractive term, σ is the hard-sphere diameter, δ is the center to center potential at u(r) = ∞, and d is the rigid-core radius.

Partial charges of tube−molecule in the equilibrium tube−molecule distance were evaluated by the natural bond orbital (NBO) calculations. Moreover, Figure 2 shows the change in the partial charges of the C atoms of the tubes vs tube−molecule distance at each step. Also, from NBO calculations, highest-occupied molecular orbital (HOMO) and lowest-unoccupied molecular orbital (LUMO) energies, natural atomic orbital occupancies, and energy of natural atomic orbital in the equilibrium tube−molecule distances were obtained.

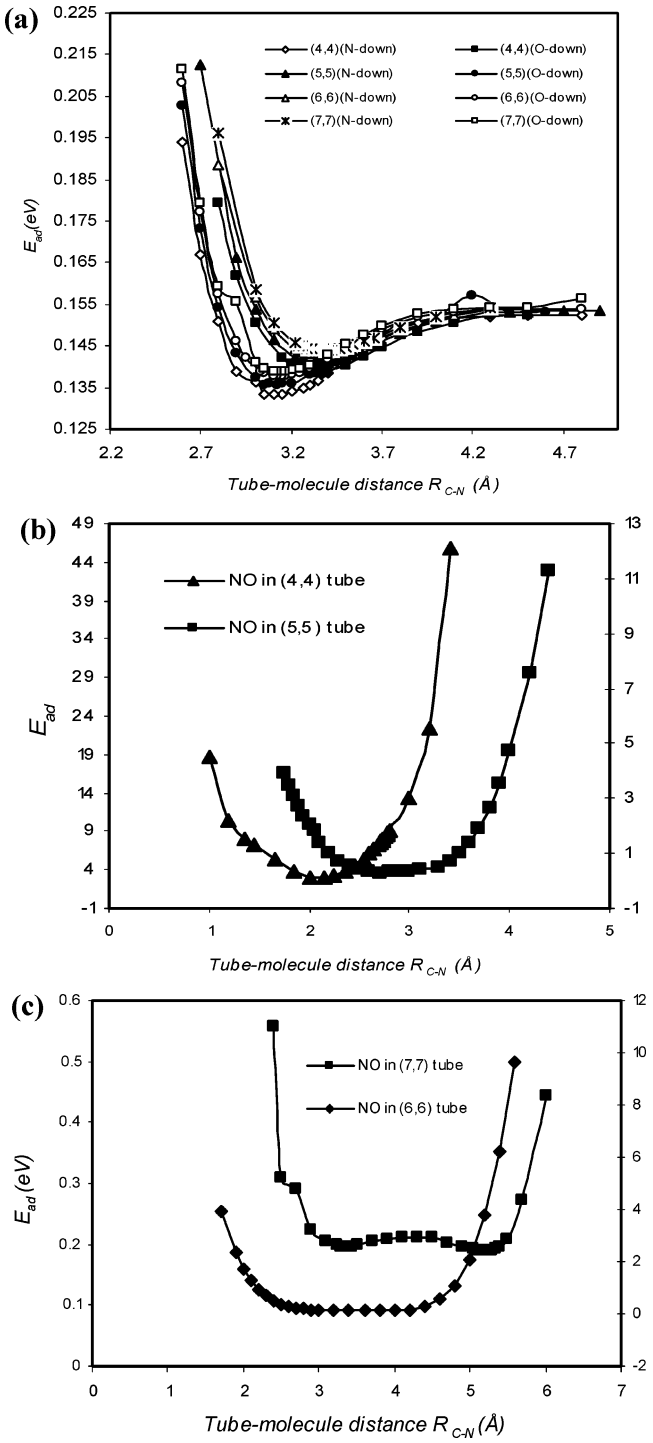

Figure 1. Adsorption energy (eV) as function of tube−molecule distance (Å) (defined as the nearest distance between the molecule and the nanotube) for tubes (4, 4), (5, 5), (6, 6), and (7, 7). (a) For N-down and O-down; (b) and (c) for the inside of the tube.

Different possible orientations of the NO gas molecules for adsorption on top of the carbon atoms of the SWNTs on the outside of the tubes were considered (the NO bond axis being perpendicular to the C atoms on the surface of the SWNTs). Also the adsorption of NO molecules on the inside of the carbon nanotubes (NO molecules perpendicular to the z axis of the tubes) was investigated (see Figure 3).

The study was done for the physisorption (the process whereby the molecules are stabilized on the outside and inside of the tubes without any type of chemical bonding between the molecules and the carbon nanotubes). Chemical potential (μ)

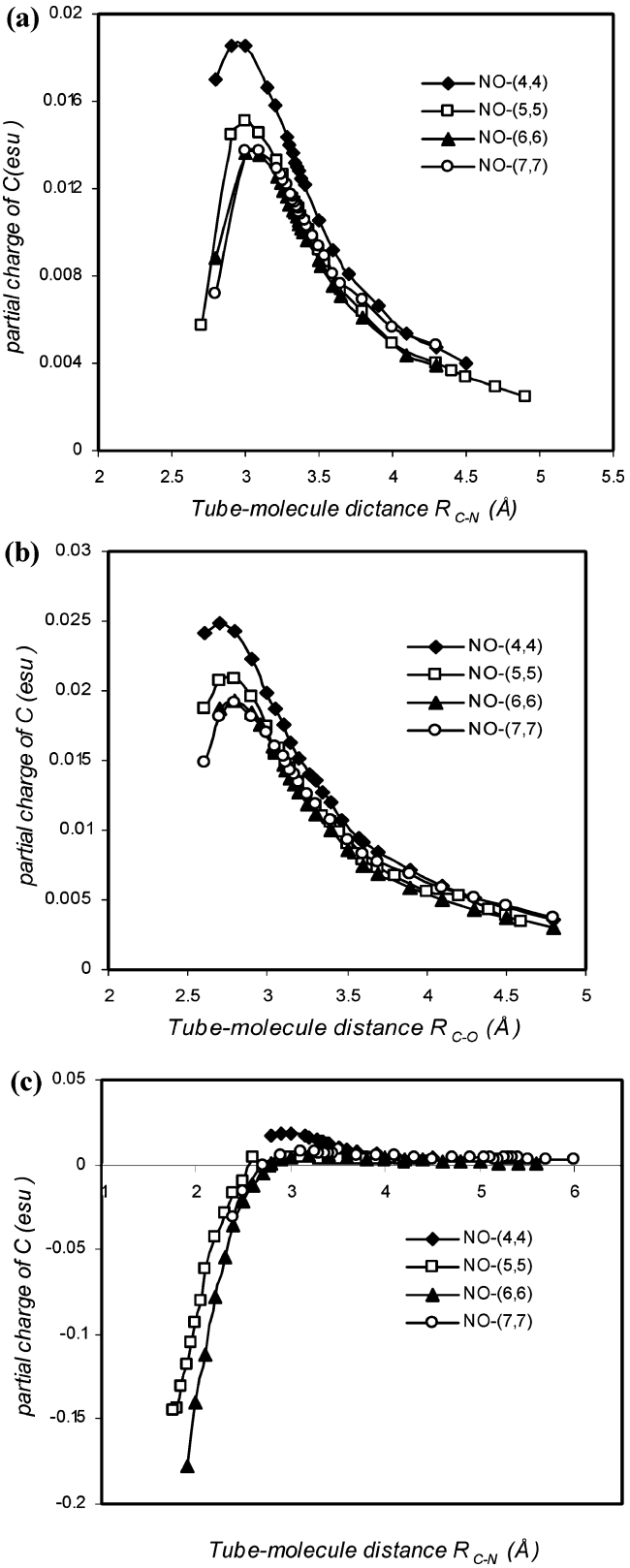

Figure 2. Partial charge of C atom vs tube−molecule distance: (a) N-down, (b) O-down, and (c) inside of the tube. *R* is defined as the nearest between the molecule and nanotube.

was calculated as half of the energy of the Fermi level (E_{HOMO}) plus the first eigenvalue of the valance band (E_{LUMO}) as follows

$$\mu = \frac{(E_{HOMO} + E_{LUMO})}{2} \tag{7}$$

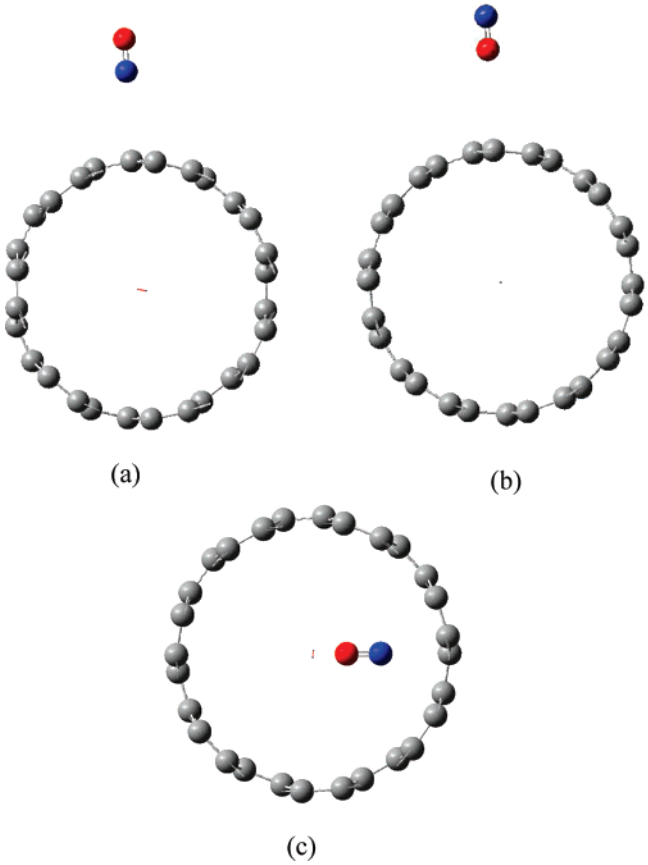

Figure 3. Geometric structures for NO adsorbed on (7, 7): (a) N-down, (b) O-down, and (c) inside of the SWNTs.

This definition was driven from eq 1. The operational definition of hardness (η) was obtained by using a finite difference approximation to the second derivative in eq 2 as[46]

$$\eta = \frac{(I - A)}{2} \tag{8}$$

where *I* and *A* are the ionization potential and electron affinity of the system, respectively. Equation 8 could be further approximated as follows, using the Koopmans' theorem[47]

$$\eta = \frac{(E_{LUMO} - E_{HOMO})}{2} \tag{9}$$

hard molecules thus have a large HOMO−LUMO gap and soft molecules have a small one.[46]

Results and Discussion

To study the adsorption of NO molecules on the walls of the carbon nanotubes, different adsorption configurations were considered for their interactions with the armchair (4, 4), (5, 5), (6, 6), and (7, 7) SWNTs: two orientations of the NO gas molecules adsorbed on the outside of the carbon nanotubes (the N-down and O-down modes) and one case for their adsorption on the inside of the carbon nanotubes (NO perpendicular to the *z* axis of the tubes). Tables 1 and 2 summarize our results on the equilibrium tube−molecule distance, adsorption energy, HOMO, LUMO, and energy gap for adsorption of NO molecules on the outside and inside of the (4, 4), (5, 5), (6, 6), and (7, 7) SWNTs. To examine the binding properties of these tubes, we calculated the total energy of the tube−molecule as well as

TABLE 1: Equilibrium Tube−Molecule Distance (R)[a], Diameter of Nanotubes (d), Adsorption Energy (E_{ad}), HOMO and LUMO Energies, and HOMO−LUMO Gap Energies of NO Molecule Adsorption on (4, 4), (5, 5), (6, 6) and (7, 7) Nanotubes (Different Possible Orientations of NO Molecule to Adsorption on Top of the Carbon Atom on the Outside of Carbon Nanotubes Are Given in the Table)

species	d (Å)	R (Å)	E_{ad} (eV)	HOMO (eV)	LUMO (eV)	gap energy (eV)
NO				−5.7620	−2.7815	2.9805
(4, 4)	5.386			−6.7414	−1.9451	4.7963
(4,4)-NO		3.30 (N-down)	0.13856	−5.5092	−2.0460	3.4632
		3.15 (O-down)	0.13322	−5.4956	−2.0136	3.4820
(5, 5)	6.732			−7.0488	−1.8428	5.2060
(5,5)-NO		3.36 (N-down)	0.14101	−5.5250	−1.9138	3.6112
		3.12 (O-down)	0.13573	−5.5166	−1.8939	3.6227
(6, 6)	8.079			−7.2725	−1.8368	5.4357
(6,6)-NO		3.32 (N-down)	0.14310	−5.5492	−1.8558	3.6934
		3.12 (O-down)	0.13768	−5.5318	−1.8384	3.6934
(7, 7)	9.425			−7.3348	−1.7867	5.5481
(7,7)-NO		3.42 (N-down)	0.14413	−5.5364	−1.8428	3.6937
		3.15 (O-down)	0.13879	−5.5536	−1.8204	3.7331

[a] Tube−molecule distance R is defined as the nearest distance between the N atom of the NO molecule and the C atom of nanotubes (N-down) and also in the other orientation of NO molecule, the nearest distance between the O atom of the NO molecule and the C atom of nanotubes (O-down).

TABLE 2: Equilibrium Tube−Molecule Distance (R)[a] (Distance between N and C Atoms), Adsorption Energy (E_{ad}), HOMO and LUMO Energies, and HOMO− LUMO Gap Energies of NO Molecule during Adsorption Inside (4, 4), (5, 5), (6, 6), and (7, 7) Nanotubes

species	R (Å)	E_{ad} (eV)	HOMO (eV)	LUMO (eV)	gap energy (eV)
(4,4)-NO	2.15 (N−C)	2.92410	−5.5092	−2.0460	3.4632
(5,5)-NO	2.70 (N−C)	0.24978	−5.5756	−2.0419	3.5337
(6,6)-NO	3.60 (N−C)	0.11148	−5.5759	−1.7619	3.8140
(7,7)-NO	5.20 (N−C)	0.18831	−5.5245	−1.7921	3.7324

[a] Tube−molecule distance R is defined as the nearest distance between the N atom of the NO molecule and the C atom of the nanotube. In this case, the NO atom is perpendicular to the z axis of nanotube.

the pristine tube and NO molecule. The adsorption energy, E_{ad}, was calculated using the expression

$$E_{ad} = E_{(tube-NO)} - (E_{tube} + E_{NO}) \quad (10)$$

The calculated adsorption energies for the different adsorption sites are summarized in Table 1, together with the corresponding structural parameters. The average distance of the N and O atoms of an NO molecule from the nearest nanotube carbon atom was about 3.12−3.42 Å. These results are consistent with the results reported by S. Irle and his co-workers.[48]

The data shown in Tables 1 and 2 contain some interesting features. First, all the calculated adsorption energies are positive. As defined by eq 10, this means that the adsorption of the NO molecules is endothermic for all the tubes. In general, NO molecules are weakly bound to the nanotubes and the tube−molecule interactions can be identified as physisorption. Second, for each tube−molecule, it can be seen that the interaction of the outside of the tubes with the O-down mode has smaller adsorption energy, so the system is more stable than the N-down mode; this is consistent with the observation that R_{C-O} is always smaller than R_{C-N} for each tube. With change in the tube size, the adsorption energy changed. The effect of the tube diameter on the stability of the tube−molecule is interesting. Stability of the tube−molecule decreased with increase in the tube diameter for the O-down mode as well as the N-down mode. Hence, the adsorption energy for the (4, 4)-NO system is lower than others for the N-down and O-down modes. In this case, the equilibrium distances between the tubes and the gas molecules were the same for all the tubes with the O-down interactions and had a little change when the tube diameter was changed. In the N-down mode, the same behavior for variation of distances with the tube diameter was observed. Table 2 shows the calculated adsorption energies for the adsorption of NO molecules on the inside of the tubes and the other structural parameters. The obtained results demonstrate that all the adsorption energies are positive. On the other hand, the adsorption energy is decreased with an increase in the tube diameter, which means more stability of the system. For the (4, 4)-NO system, this value is more positive, implying that, for the tubes with the lowest diameter, NO molecules cannot settle inside the tubes (perpendicular to the z axis of the tubes). So, in this case, at the equilibrium tube−molecule distance, the nearest distance between the O atoms of NO molecules and the C atoms of the nanotubes was changed with change in the SWNT size. For the (4, 4)-NO system, R_{C-O} was the lowest and for the (7, 7)-NO system, it was the highest. These results can denote the effect of the tube diameter on the stability of the tubes. Also for the (7, 7) tube with a large diameter, this effect disappeared. A comparison between the results obtained for the outside and inside of the tubes indicates that the effect of the tube diameter on the adsorption energy is different. For the outside adsorption, E_{ad} decreased with increase in the tube diameter, while for the inside adsorption, E_{ad} increased with increase in the tube diameter. Moreover, for tubes of 8 Å diameters, adsorption on the inside of the tubes shows lower E_{ad} values than the other cases.

TABLE 3: Attractive Term (ϵ), Hard-Sphere Diameter (σ), Center to Center Potential at $u(r) = \infty$ and Rigid-Core Radius (d) for All Outside Adsorption Modes

species	orientation	ϵ (eV)	σ (Å)	δ (Å)	d (Å)
(4,4)-NO	N-down	0.01397	2.940	2.975	0.675
	O-down	0.01919	2.806	2.790	0.650
(5,5)-NO	N-down	0.01240	2.993	3.010	0.675
	O-down	0.01738	2.778	2.808	0.650
(6,6)-NO	N-down	0.01057	2.958	3.014	0.675
	O-down	0.01616	2.780	2.827	0.650
(7,7)-NO	N-down	0.00999	3.045	3.03	0.675
	O-down	0.01745	2.806	2.889	0.650

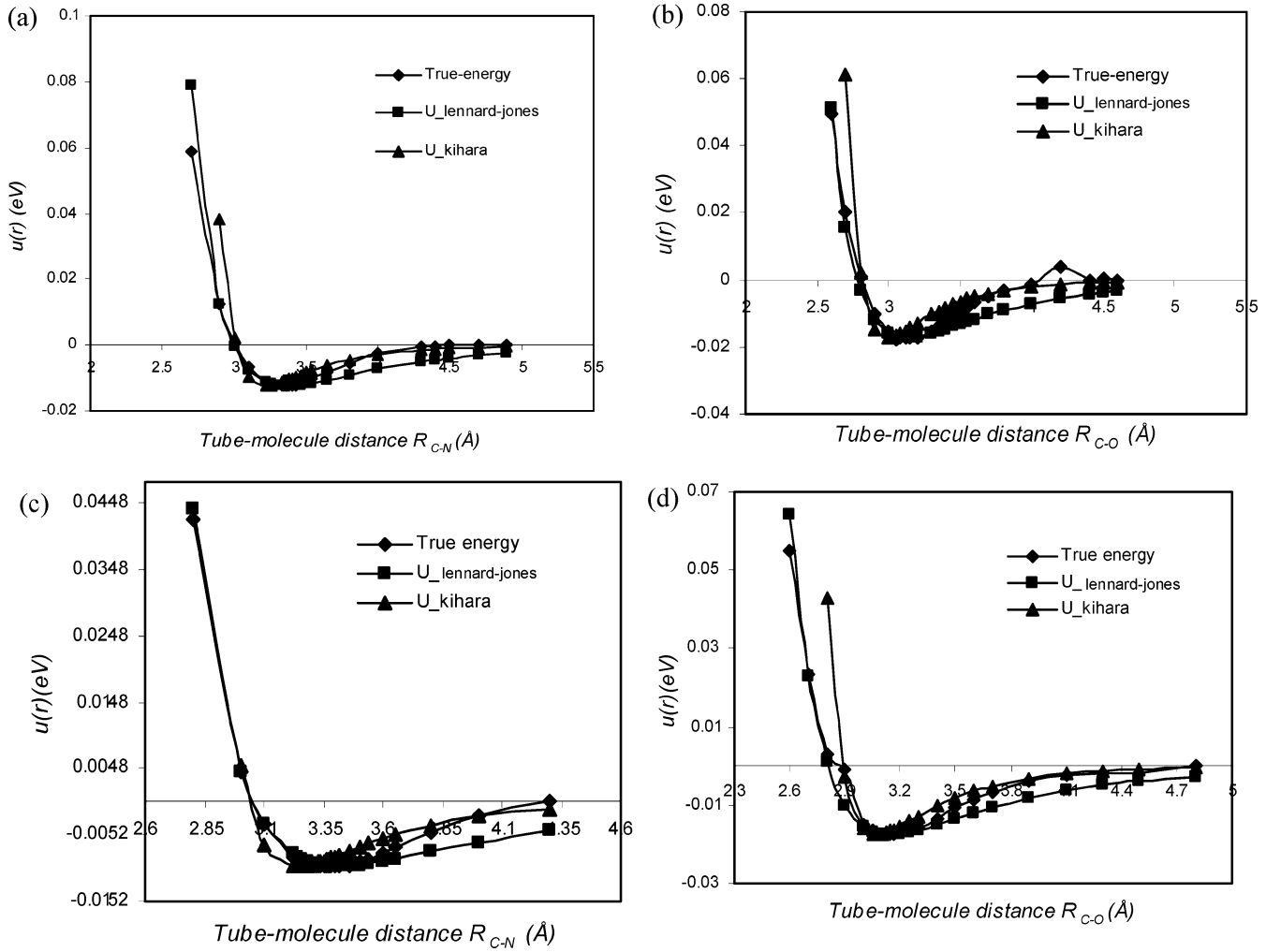

Figure 4. Typically Fitted potential energy curves (true energy) with two potential equations for the (5, 5)-NO system, (a) N-down and (b) O-down; for the (7, 7)-NO system, (c) N-down and (d) O-down system, respectively.

All adsorption energy curves for outside of the tubes were fitted with two potential equations, Lennard-Jones and Kihara, to obtain the parameters of these equations. For the inside of the carbon nanotubes, we could not fit the adsorption energy curves with the potential equations. The results obtained are listed in Table 3. (These data were used to perform a Monte Carlo simulation of adsorption of gases on nanotubes and will be published later). Figure 4 shows the fitted potential energy curves (true energy) with two potential equations. These curves show the typical features of intermolecular interactions. These results reflect the salient features of real interactions in a general way. These potential energy curves also illustrate a simple Lennard-Jones 12−6 potential, which provides a reasonable description of the properties of the tube−molecules, via computer simulation, if the parameters ϵ and σ are used. The potential has a long-range attractive portion of the form $-1/r^6$, a negative well of depth ϵ, and a steeply rising repulsive wall at distances less than $r \approx \sigma$. The fitted potential data show that the long-range attractive portion has more correlation with the Kihara potential than with the Lennard-Jones potential, while the short-range repulsive portion has a better correlation with the Lennard-Jones potential than with the Kihara potential.

Figure 5 shows the plot of the HOMO−LUMO gap vs diameters (d) of the tubes for the N-down and O-down modes. As it could be observed in the figure, the energy gap increases monotonically with increase in the tube diameter for the outside and inside of the tubes, but after $d > 9$ Å, the energy gap approaches the ∼3.7-eV value. A comparison between the O-down and N-down modes for the HOMO−LUMO gap indicates that the energy gap for the O-down mode is higher than that for the N-down mode. According to the difference between the frontier orbitals energies when the energy gap is higher, the system behaves like a very stable molecule. In addition, the high HOMO energy indicates that the molecule can undergo an electrophilic attack with a large probability.

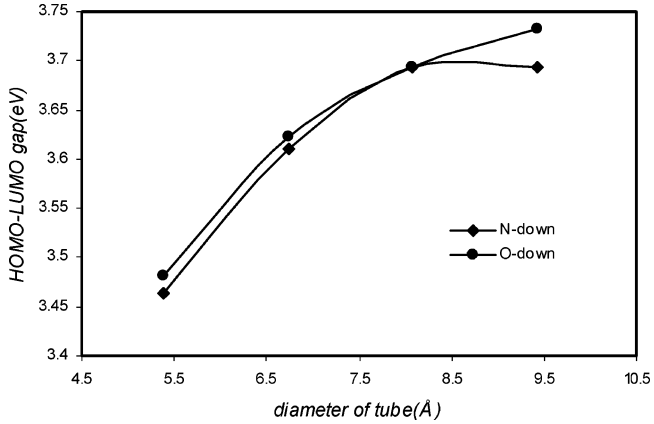

Figure 5. HOMO−LUMO gap energy (eV) vs diameter (d) of (4, 4), (5, 5), (6, 6), and (7, 7) tubes for N-down and O-down modes.

Three-dimensional pictures of the HOMO of the valance band and the LUMO of a conduction band for the (4, 4) tube−

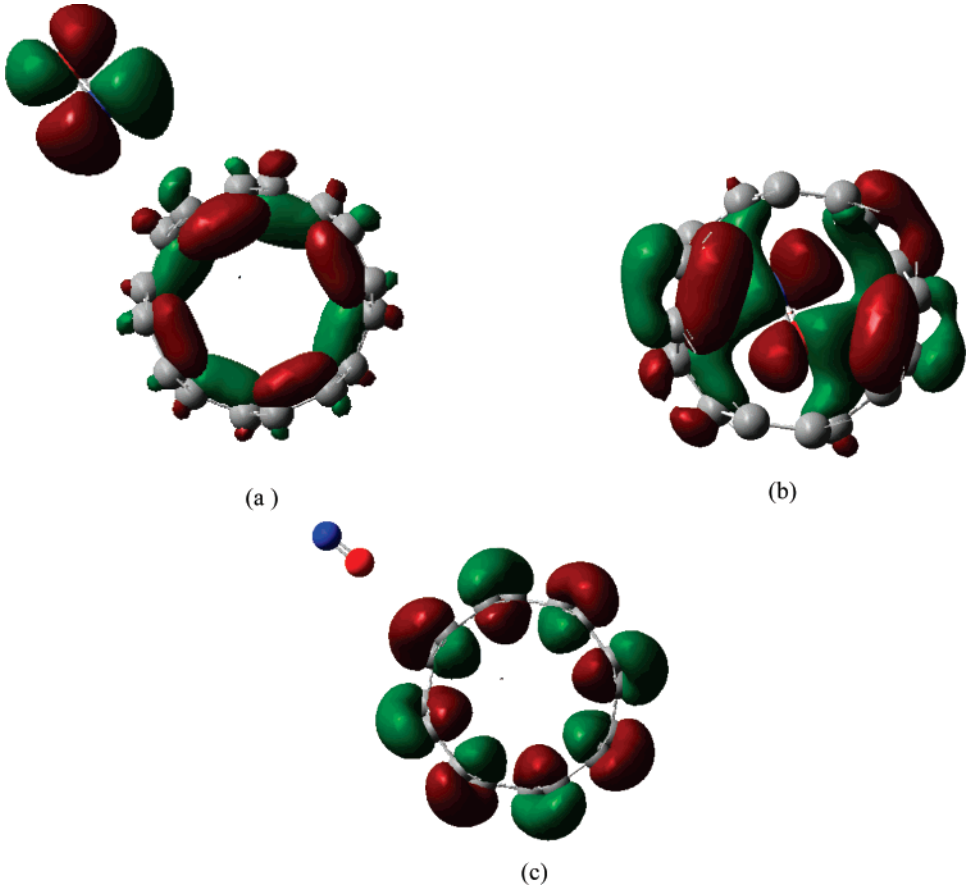

Figure 6. Contour plots of HOMO−LUMO for tube (4, 4)-NO system: (a) N-down, (b) inside of the tube, and (c) O-down.

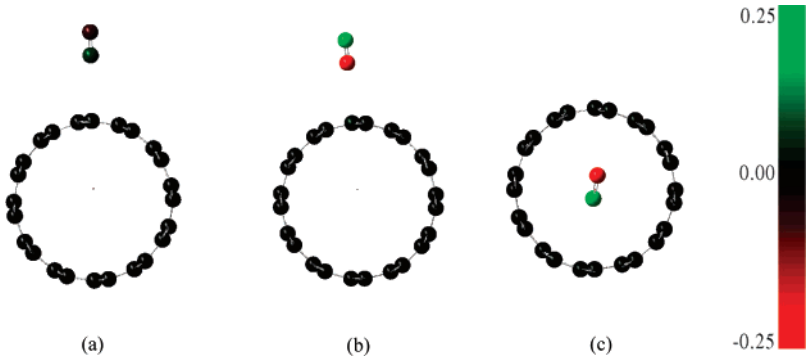

Figure 7. Schematic structures and Mulliken atomic charge populations of tube (6, 6) and NO gas molecule: (a) N-down, (b) O-down, (c) inside. The colors of the atoms show the Mulliken atomic charge amount in electrons.

molecule are presented in Figure 6. The physisorption process for all the systems occurred at the 3.12−3.42 Å distance from the surface of the tube, namely, between N or O atom and the closest C atom on top of the surface of the tubes. As it could be observed in Figure 6, neither the HOMO nor the LUMO present a contribution from the NO molecules. In addition, Table 4 shows the natural atomic orbital (AO) occupancies and their energies (eV) in the equilibrium tube−molecule distances for α spin orbitals of carbon atom for all the systems in the three modes (inside, N-down, O-down, and inside of the tubes). The global indices of reactivity in the context of DFT are presented in Table 5. An NO molecule displays the lowest hardness value (1.49023 eV), which is related to the lowest stability of this molecule. By considering the frontier orbital energies of NO molecule (the energy gap of this molecule approximately to 2.98047 eV), this molecule behaves like an unstable molecule. The value of hardness, softness, electerophilicity and chemical potential for tube−molecule is differing from the individual tube and NO molecule. In the presence of NO as a molecule interacting with carbon nanotube, the capacity of carbon nanotube to attract electrons was diminished and the hardness of the molecule was decreased, which means decreased stability of the system. In addition, as the hardness of the carbon nanotubes is larger than the tube−molecule system, we can predict that the tubes are relatively stable and a physisorption process is dominant. These results are consistent with the results of adsorption energy of tube−molecule. A comparison between the O-down and N-down modes show that all local indices for the O-down mode are higher than those for the N-down mode. Hence the O-down mode is more stable than the N-down mode.

For the inside of the carbon nanotubes, the results are quite similar to the results for the N-down mode. Figure 2 shows the results of the Mulliken population analysis of the charged for N-down, O-down mode and inside of the tubes. When NO molecules and carbon nanotubes interact to give the tube−molecule system, there is a charge-transfer producing a common

TABLE 4: Natural Atomic Orbital (AO) Occupancies and Energy (eV) of Atomic Orbital in Equilibrium Tube−Molecule Distances for α Spin Orbitals of Carbon Atom for All Systems in Three Modes (N-Down and O-Down)

type	type (AO)	occupancy	energy
	(4, 4) (N-down)		
C	Val (2S)	0.68172	−51.8274
C	Val (2px)	0.11768	−23.6277
	(4, 4) (inside)		
C	Val (2S)	0.71866	−66.897
C	Val (2px)	0.11952	−23.5501
	(4, 4) (O-down)		
C	Val (2S)	0.68178	−51.7599
C	Val (2px)	0.11772	−23.6007
	(5, 5) (N-down)		
C	Val (2S)	0.69510	−45.7522
C	Val (2px)	0.11215	−23.6059
	(5, 5) (inside)		
C	Val (2S)	0.69968	−43.0087
C	Val (2px)	0.11098	−23.4336
	(5, 5) (O-down)		
C	Val (2S)	0.69490	−45.6313
C	Val (2px)	0.11204	−23.5686
	(6, 6) (N-down)		
C	Val (2S)	0.70845	−39.5346
C	Val (2px)	0.11298	−23.5629
	(6, 6) (inside)		
C	Val (2S)	0.70879	−39.696
C	Val (2px)	0.11349	−23.4957
	(6, 6) (O-down)		
C	Val (2S)	0.70792	−39.5417
C	Val (2px)	0.11294	−23.5294
	(7, 7) (N-down)		
C	Val (2S)	0.68960	−46.5018
C	Val (2px)	0.11364	−23.5417
	(7, 7) (inside)		
C	Val (2S)	0.69147	−46.7481
C	Val (2px)	0.11365	−23.546
	(7, 7) (O-down)		
C	Val (2S)	0.68942	−46.4047
C	Val (2px)	0.11360	−23.5014

TABLE 5: Chemical Potential (μ), Tube−Molecule Distance (R), Hardness (η), Softness (S), and Electrophilicity (w) of the NO Molecule and Tubes and for Tube−Molecule Outside and Inside of the (4, 4), (5, 5), (6, 6), and (7, 7) Carbon Nanotubes

species	R (Å)	μ (eV)	η (eV)	S (1/eV)	w (eV)
NO		−4.2718	1.4902	0.33552	6.1226
(4, 4)		−4.3432	2.3981	0.20850	3.9329
(4, 4)-NO	3.30 (N-down)	−3.7776	1.7316	0.28875	4.1206
	3.15 (O-down)	−3.7546	1.7410	0.28719	4.0486
	2.15(inside)	−3.7776	1.7316	0.28875	4.1206
(5, 5)		−4.4458	2.6030	0.19208	3.7965
(5, 5)-NO	3.36 (N-down)	−3.7194	1.8056	0.27692	3.8308
	3.12 (O-down)	−3.7052	1.8113	0.27604	3.7897
	2.70(inside)	−3.8088	1.7668	0.28300	4.1053
(6, 6)		−4.5546	2.7179	0.18397	3.8164
(6, 6)-NO	3.32 (N-down)	−3.7025	1.8467	0.27075	3.7117
	3.12 (O-down)	−3.6851	1.8467	0.27075	3.6768
	3.6 (inside)	−3.6689	1.9070	0.26220	3.5294
(7,7)		−4.5608	2.7741	0.18024	3.7491
(7, 7)-NO	3.42 (N-down)	−3.6896	1.8468	0.27073	3.6855
	3.15 (O-down)	−3.6870	1.8666	0.26787	3.6415
	5.20 (inside)	−3.6583	1.8662	0.26793	3.5858

chemical potential. For the N-down and O-down modes, parts a and b of Figure 2 show that the partial charges on the C atoms are positive. Partial charges of the C atoms increase with decrease in R_{C-N} or R_{C-O}. In addition, after the 2.7−2.9 Å distance, partial charges of the C atoms decrease with the decrease in R_{C-N} or R_{C-O}. For the inside adsorption case, partial charges on the C atoms are negative, but when R_{C-N} is larger than 2.8−2.9 Å, this quantity shifts to positive values. In all cases, the partial charges on the N atoms were positive and those for the O atoms were negative. In addition, for the O-down mode, the partial charges on the N atoms were greater than those in the N-down mode. The Mulliken atomic charges of the C, N, and O atoms in the equilibrium geometry are tabulated in Table 6. The Mulliken atomic charge populations of the (6, 6)-NO system are given in Figure 7. These may explain the different behaviors of the NO adsorption on the SWNTs.

TABLE 6: Partial Charges (esu) of C, N, O Atoms for Adsorption of NO on (4, 4), (5, 5), (6, 6), and (7, 7) Carbon Nanotubes at Equilibrium Tube−Molecule Distances

	N atom	O atom	C atom
	N-down		
NO-(4,4) tube	0.191855	−0.212867	0.014000
NO-(5,5) tube	0.194290	−0.211656	0.011045
NO-(6,6) tube	0.194803	−0.211776	0.011241
NO-(7,7) tube	0.197642	−0.209718	0.010542
	O-down		
NO-(4,4) tube	0.199590	−0.219551	0.016246
NO-(5,5) tube	0.200277	−0.218422	0.014762
NO-(6,6) tube	0.201888	−0.217009	0.014304
NO-(7,7) tube	0.200601	−0.217129	0.014296
	Inside Tube		
NO-(4,4) tube	0.264644	−0.271090	−0.081369
NO-(5,5) tube	0.192571	−0.233005	0.004977
NO-(6,6) tube	0.187259	−0.222769	0.003797
NO-(7,7) tube	0.197035	−0.219927	0.000538

The C atoms in the N-down, O-down, and inside geometry modes are colored in black, suggesting that their charges are positive, and the other C atoms at equilibrium geometries are marked in dark green, indicating that they have small positive charges. The atoms colored in black are electroneutral. The colors of N atoms are distinct, namely, light green and dark green, implying that the N atoms are positively charged. Regarding the electron transfers, the C and N atoms are electron donors. The addition of O atoms leads to a different behavior. O atoms, light red colored, are negatively charged, suggesting an inverse electron transfer. Therefore, it seems that the electrostatic force between the C atoms of tubes and the O atoms is an attractive one. The results show that an NO molecule is a charge acceptor and that the charge transfer is not negligible.

Conclusion

We used the DFT in conjugation with the periodic boundary condition to study the interactions of some armchair SWNTs with NO molecule. The energy values and the equilibrium distances between the O or N and C atoms (R_{C-N} and R_{C-O}) obtained from the DFT calculations are typical of physisorption.

The following results were obtained in the study of NO adsorption on a series of armchair SWNTs:

(1) Adsorptions occurred on the outside and inside of the nanotubes. In the outside adsorption, NO molecules could be adsorbed via the N-down or O-down mode. The adsorption energies obtained show that the O-down mode is more stable than the N-down mode. On the other hand, stability of the system for the outside is more than that for the inside adsorption process.

(2) The data obtained at equilibrium tube−molecule distance show that stability of the system decreases with increase in the tube diameter for the outside adsorption process. So the (4, 4)−

NO system is more stable than the other systems. To the contrary, for the inside adsorption process, the stability of the system increases with increasing nanotube diameter up to 8.5 Å. After this diameter, the stability does not change with changing the nanotube diameter.

(3) Finally we found that adsorption of NO molecules on SWNTs is accompanied with small charge transfer, so NO molecules are weakly adsorbed on SWNTs. Also NBO calculations essentially show significant change in the nanotube band gap when NO molecules approach the nanotubes.

References and Notes

(1) Tada, K.; Furuya, S.; Watanabe, K. *Phys. Rev. B* **2001**, *63*, 155405−155409.
(2) Buldum, J. Z. A.; Han, J.; Lu, J. P. *Nanotechnology* **2002**, *13*, 195−200.
(3) Ulbricht, H.; Moos, G.; Hertel, T. *Phys. Rev. B* **2002**, *66*, 075404−075411.
(4) Fischer, J. E. *Chem. Innov.* **2000**, *30*, 21−27.
(5) Meunier, V.; Kephart, J.; Roland, C.; Bernholc, J. *Phys. Rev. Lett.* **2002**, *88*, 075506−075509.
(6) Dresselhaus, M. S.; Dressehaus, G.; Eklund, P. C. *Science of fullerenes and Carbon Nanotubes*; Academic: New York, 1996.
(7) Ebbesen, T. *Carbon Nanotube: Preparation and Properties*; Boca Raton, Fl: CRC Press, 1997.
(8) Saito, R.; Dresselhaus, G.; Dresselhaus, M. S. *Physical Properties of Carbon Nanotubes*; Imperial College Press: London, UK, 2001.
(9) Zhao, J.; Buldum, A.; Han, J.; Lu, J. P. *Phys. Rev. Lett.* **2000**, *85*, 1706−1709.
(10) (a) Dillon, A. C.; Jones, K. M.; Bekkedahl, T. A.; Kiang, C. H.; Bethune, D. S.; Heben, M. J. *Nature (London)* **1997**, *386*, 377−379. (b) Hirscher M.; Becher, M.; Haluska, M.; Dettlaff-Weglikowska, U.; Quintel, A.; Duesberg, G. S.; Choi, Y. M.; Downes, P.; Hulman, M.; Roth, S.; Stepanek, I.; Bernier, P. *Appl. Phys. A.* **2001**, *79*, 129−132.
(11) Collins, P. G.; Bradley, K.; Ishigami, M.; Zettl, A. *Science* **2000**, *287*, 1801−1804.
(12) Kong, J.; Franklin, N. R.; Zhou, C.; Chapline, M. G.; Peng, S.; Cho, K.; Dai, H. *Science* **2000**, *287*, 622−625.
(13) Dag, S.; Gulseren, O.; Ciraci, S. *Chem. Phys. Lett.* **2003**, *380*, 1−5.
(14) Fujitani, T.; Nakamura, L.; Kobayashi, Y.; Takahashi, A.; Haneda, M.; Hamada, H. *J. Phys. Chem. B* **2005**, *109*, 17603−17607.
(15) Liu, H. J.; Chan, C. T.; Liu, Z. Y.; Shi, J. *Phys. Rev. B* **2005**, *72*, 075435−075439.
(16) Tang, X. P.; Kleinhammes, A.; Shimoda, H.; Fleming, L.; Bennouse, K. Y.; Sinha, S.; Bower, C.; Zhou, O.; Wu, Y. *Science* **2000**, *288*, 492−494.
(17) Jhi, H.; Loui, S. G.; Cohen, M. L. *Phys. Rev. Lett.* **2000**, *85*, 1710−1713.
(18) Chan, P.; Chen, G.; Gong, X. G.; Liu, Z. F. *Phys. Rev. Lett.* **2003**, *90*, 086403−086404.
(19) Park, N.; Han, S. W.; Ihm, J. *Phys. Rev. B* **2001**, *64*, 125401−125404.
(20) Froudakis, G. E.; Schnell, M.; Muhlhauser, M.; Peyerimhoff, S. D.; Andriotis, A. N.; Menon, M.; Sheetz, R. M. *Phys. Rev. B* **2003**, *68*, 115435−115439.
(21) Ricca, A.; Bauschlicher, C. W. *Phys. Rev. B* **2003**, *68*, 035433−035439.
(22) Zhu, X. Y.; Lee, S. M.; Lee, Y. H.; Frauenheim, T. *Phys. Rev. Lett.* **2000**, *85*, 2757−2760.
(23) Giannozzi, P.; Car, R.; Scoles, G. *J. Chem. Phys.* **2003**, *118*, 1003−1006.
(24) Scorescu, D. C.; Jordan, K. D. *J. Phys. Chem. B* **2001**, *105*, 11227−11232.
(25) Kyotani, T.; Tomita, A. *J. Phys. Chem. B* **1999**, *103*, 3434−3441.
(26) Byl, O.; Kondratyuk, P.; Yates, J. T. *J. Phys. Chem. B* **2003**, *107*, 4277−4279.
(27) Orita, H.; Nakamura, I.; Fujitani, T. *J. Phys. Chem. B* **2005**, *109*, 10312−10318.
(28) Tabata, K.; Kamada, M.; Choso, T.; Munakata, H. *J. Phys. Chem. B* **1997**, *101*, 9161−9164.
(29) Lu, X.; Xu, X.; Wang, N.; Zhang, Q. *J. Phys. Chem. B* **1999**, *103*, 5657−5664.
(30) Brand, H. V.; Redondo, A.; Hay, P. J. *J. Phys. Chem. B* **1997**, *101*, 7691−7701.
(31) Parr, R. G.; Yang, W. *Density Functional Theory of Atoms and Molecules*; Oxford University Press: New York, 1989.
(32) Sen, K. D.; Jorgensen, C. K. *Electronegativity, Structure and Bonding*; Springer-Verlag: New York, 1987; No. 66.
(33) Gomez, B.; Martinez-Magadan, J. M. *J. Phys. Chem. B* **2005**, *109*, 14868−14875.
(34) Chattara, P. K.; Poddar, A. *J. Phys. Chem. B* **1999**, *103*, 1274−1275.
(35) Pearson, R. G. *Chemical Hardness: Applications from Molecules to Solids*; Wiley-VCH Verlag GMBH: Weinheim, Germany, 1997.
(36) Yang, W.; Parr, R. G. *Proc. Natl. Acad. Sci. U.S.A* **1985**, *82*, 6723−6726.
(37) Parr, R. G.; Yang, W. *J. Am. Chem. Soc*. **1984**, *106*, 4049−4050.
(38) (a) Pearson, R. G. *Hard and Soft Acid and Bases*; Dowden, Hutchinson and Ross: Stroudsberg, PA, 1973. (b) Pearson, R. G. *J. Am. Chem. Soc.* **1963**, *85*, 3533−3539.
(39) Pearson, R. G. *J. Chem. Educ.* **1987**, *64*, 561−567.
(40) Ayers, P. W.; Parr, R. G. *J. Am. Chem. Soc.* **2000**, *122*, 2010−2018.
(41) Pearson, R. G. *Acc. Chem. Res.* **1993**, *26*, 250−255.
(42) Pearson, R. G.; Donnelly, R. A.; Levy, M.; Palke, W. E. *J. Chem. Phys.* **1978**, *68*, 3801−3807.
(43) Parr, R. G.; Pearson, R. G. *J. Am. Chem. Soc.* **1983**, *105*, 7512−7516.
(44) Pearson, R. G.; Szentpaly, L.; Liu, S. *J. Am. Chem. Soc.* **1999**, *121*, 1922−1924.
(45) Frisch, M. J.; Trucks, G. W.; Schlegel, H. B.; Scuseria, G. E.; Robb, M. A.; Cheeseman, J. R.; Montgomery, J. A.; Vreven, J. T.; Kudin, K. N.; Burant, J. C.; Millam, J. M.; Iyengar, S. S.; Tomasi, J.; Barone, V.; Mennucci, B.; Cossi, M.; Scalmani, G.; Rega, N.; Petersson, G. A.; Nakatsuji, H.; Hada, M.; Ehara, M.; Toyota, K.; Fukuda, R.; Hasegawa, J.; Ishida, M.; Nakajima, T.; Honda, Y.; Kitao, O.; Nakai, H.; Klene, M.; Li, X.; Knox, J. E.; Hratchian, H. P; Cross, J. B.; Adamo, C.; Jaramillo, J.; Gomperts, R.; Stratmann, R. E.; Yazyev, O.; Austin, A. J.; Cammi, R.; Pomelli, C.; Ochterski, J. W.; Ayala, P. Y.; Morokuma, K.; Voth, G. A.; Salvador, P.; Dannenberg, J. J.; Zakrzewski, V. G.; Dapprich, S.; Daniels, A. D.; Strain, M. C.; Farkas, O.; Malick, D. K.; Rabuck, A. D.; Raghavachari, K.; Foresman, J. B.; Ortiz, J. V.; Cui, Q.; Baboul, A. G.; Clifford, S.; Cioslowski, J.; Stefanov, B. B.; Liu, G.; Liashenko, A.; Piskorz, P.; Komaromi, I.; Martin, R. L.; Fox, D. J.; Keith, T.; Al-Laham, M. A.; Peng, C. Y.; Nanayakkara, A.; Challacombe, M.; Gill, P. M. W.; Johnson, B.; Chen, W.; Wong, M. W.; Gonzalez, C.; Pople, J. A. *Gaussian 03*; Gaussian, Inc., Pittsburgh, PA, 2003.
(46) Pearson, R. G. *Inorg. Chem.* **1988**, *27*, 734−740.
(47) Chattaraj, P. K.; Poddar, A. *J. Phys. Chem. A* **1999**, *103*, 8691.
(48) Xu, S. C.; Irle. S.; Musaev, D. G.; Lin, M. C. *J. Phys. Chem. B* **2006**, *110*, 21135−21144.